Scientific Research Publishing

Determination of Bonding Failures in Transparent Materials with Non-Destructive Methods—Evaluation of Climatically Stressed Glued and Laminated Glass Compounds

Christin Sirtl[1], Matthias Kraus[1], Christiane Hadlich[2], Andrea Osburg[2]

[1]Department of Steel and Hybrid Structures, Bauhaus University of Weimar, Weimar, Germany
[2]Department of Building Chemistry and Polymer Materials, Bauhaus University of Weimar, Weimar, Germany
Email: christin.sirtl@uni-weimar.de

Abstract

As part of an international research project—funded by the European Union—capillary glasses for facades are being developed exploiting storage energy by means of fluids flowing through the capillaries. To meet highest visual demands, acrylate adhesives and EVA films are tested as possible bonding materials for the glass setup. Especially non-destructive methods (visual analysis, analysis of birefringent properties and computed tomographic data) are applied to evaluate failure patterns as well as the long-term behavior considering climatic influences. The experimental investigations are presented after different loading periods, providing information of failure developments. In addition, detailed information and scientific findings on the application of computed tomographic analyses are presented.

Keywords

Non-Destructive Testing, Bonding Methods, Computed Tomography

1. Introduction

In order to meet European climate regulations [1], large facades are to be actively involved in the energy supply of buildings. The high transmission of glass panes can be utilized to harvest solar energy and to contribute to the building technology system [2].

Within the framework of a research project, rolled capillary glasses are developed to be applied in insulating glass units (IGU) as shown in **Figure 1(a)**. The
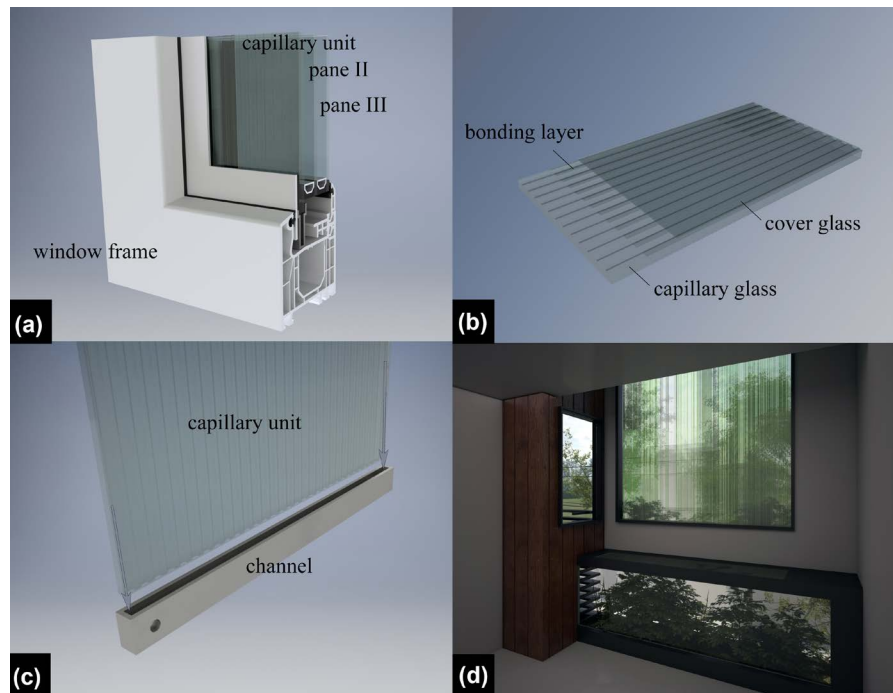
Figure 1. Capillary unit, (a) components integrated in IGU, (b) components of unit, (c) capillary unit with channel, (d) indoor view of IGU with integrated, colored capillary unit.

schematic setup of the units is presented in **Figure 1(b)**. A fluid circulating through the capillaries enables an energy/heat storage and transfer by heat exchangers. Two channels, which are arranged at the top and bottom of the pane and which are connected to the building technology system (**Figure 1(c)**), distribute the fluid to and collect it from the capillaries. Next to the energy saving and insulating function of the IGU (see **Figure 1(d)**), further applications are possible. The capillary unit can for example be used as a direct heating or cooling device in this context. It can also be applied in partition walls of offices or public buildings to contribute to a comfortable room climate. Furthermore, the employed fluid can be enhanced to a magneto-active liquid, enabling tunable shading functions (see [3]).

The bonding between capillary and cover glass has to satisfy high demands in terms of strength, transparency and durability (**Table 1**). However, the long-term behavior is influenced by atmospheric impacts (temperature change, fluid contact, UV irradiation) as well as static loads (wind suction and pressure, capillary pressure of the fluid).

At the University of Weimar, the long-term behavior of suitable bonding materials under atmospheric influences is investigated and described. With the help of non-destructive methods, the authors want to attain information on the aging process in transparent connections and on corresponding failure developments, respectively. The results will be used to improve and develop numerical models for aging plastic materials in future.

Table 1. Required criteria of bonded glass-glass connections.

Visual requirements	Long-term resistance against	Mechanical requirements
- Highly transparent joint over time - Colorless - Non-porous	- Temperature - Humidity - Fluid (glycol mixture) - UV-radiation	Durable load-bearing functioning and high adhesion of the connection in a temperature range of −20˚C to +80˚C and under fluid attack

Two different types of bonding materials are chosen for testing, namely acrylate adhesives and EVA films. UV-curing acrylate adhesives meet the visual requirements, which is one of the highest priorities in the selection of the bonding materials. In addition, an EVA film (ethylene vinyl acetate copolymer film) is tested as a bonding material. As suitable material for glass lamination [4], it is chosen for reasons of strength and high transparency, whereas the material behavior for artificial aging is to be analyzed.

2. Components and Bonding Materials

The functional capillary unit (capillary glass, bonding layer and cover glass) consists of a glass pane with capillary structure made of soda lime silicate glass (produced in float process) and of a 0.75 mm thin glass made of modified and chemically prestressed aluminosilicate glass. In the modifying process, the thermal expansion coefficient and the refractive index are adjusted to the float glass. The characteristic properties of the two glasses are compiled in Table 2.

As mentioned above, UV-curing acrylates and EVA films are tested for their possible application in the capillary unit as bonding layer. Due to the molecular structure, acrylates are assigned to thermoset providing resistance and stiffness, respectively, at serviceability temperature ranges by close-meshed polymers. The mostly one-component materials can be applied and processed without any difficulties. Regarding the experimental scheme, three acrylate urethanes (urethane systems supplemented by nitro groups) are analyzed, curing by UV radiation and polymerization within a few minutes and without any additional pressure. In the following evaluation and discussion, one of the acrylates is focused and referred to as "A" as specified in Table 3. Further details on the acrylate experiments including all test series can be found in [7].

The second material, an ethylene vinyl acetate copolymer (EVA) film, is an elastic intermediate film (elastomer) for permanent bonding of glasses. Based on ethylene vinyl acetate copolymers, a highly and three-dimensional crosslinked composite layer forms between the glasses at certain temperature exposures, which acts as basic component of composite or laminated safety glass. As non-hygroscopic material, the employed EVA product is characterized by high transparency after lamination, good adhesion to glass and easy processing by vacuum lamination or autoclaving procedures [8]. For the application of the material in laminated safety glass a technical approval is available [4]. The

Table 2. Characteristic properties of bonded components [5] [6].

Property	Float glass (capillary glass)	Modified aluminosilicate glass
Density [kg/m^3]	2500	2477
Bending tensile strength [N/mm^2]	45	200
Young's Modulus [N/mm^2]	70,000	74,000
Middle thermal coefficient of expansion [1/K]	9.0×10^{-6}	8.8×10^{-6}
Refractive index	≈1.52	1.508

Table 3. Characteristic properties of bonding materials—information based on manufacturer specifications [9] [10].

Property	Acrylate (A)	EVA (D)
Density [g/cm^3]	1.0	0.95 - 0.97
Tensile strength [N/mm^2]	33	> 20
Elongation at tear [%]	4	>700
Young's Modulus [N/mm^2]	1600	No specification
Refraction index	1503	1480

characteristic properties of the material focused in the following evaluations are compiled in Table 3, where one of two analyzed EVA films is focused referred to as experimental series "D".

3. Experimental Approach

Figure 2 presents the experimental scheme applied to several test series and specimens, respectively. Unified testing procedures for lap joint tests are specified in codes, however, generally for connecting metals [11] [12]. The design of the glass specimens is therefore adjusted to testing procedures of material manufacturers [13]. The glass components to be joined are 20 by 20 mm with thickness of 8 mm and the overlapping length is 5 mm, s. Figure 3. The thickness of the bonding layer depends on the material. For acrylates it is set to 250 μm and for the EVA films presented here to 100 μm (D).

Aging is defined as totality of physical and chemical material changes over time [14]. Various methods for characterization and quantification of these changes are distinguished [15]. On the experimental level, material aging is usually induced by accelerated artificial impacts in the sense of a time lapse [16] [17] [18]. In doing so, the artificial simulations have to be adapted from realistic environmental influences. For the tests presented here, they have to in addition meet the requirements of Table 1.

The artificial aging is customized to the environmental conditions of the capillary glass unit. A main climatic influence is provoked by temperature gradients. They are caused by different temperature levels at the inlet and outlet of the fluid (as a result of energy harvest by the fluid and its circulation) as well as
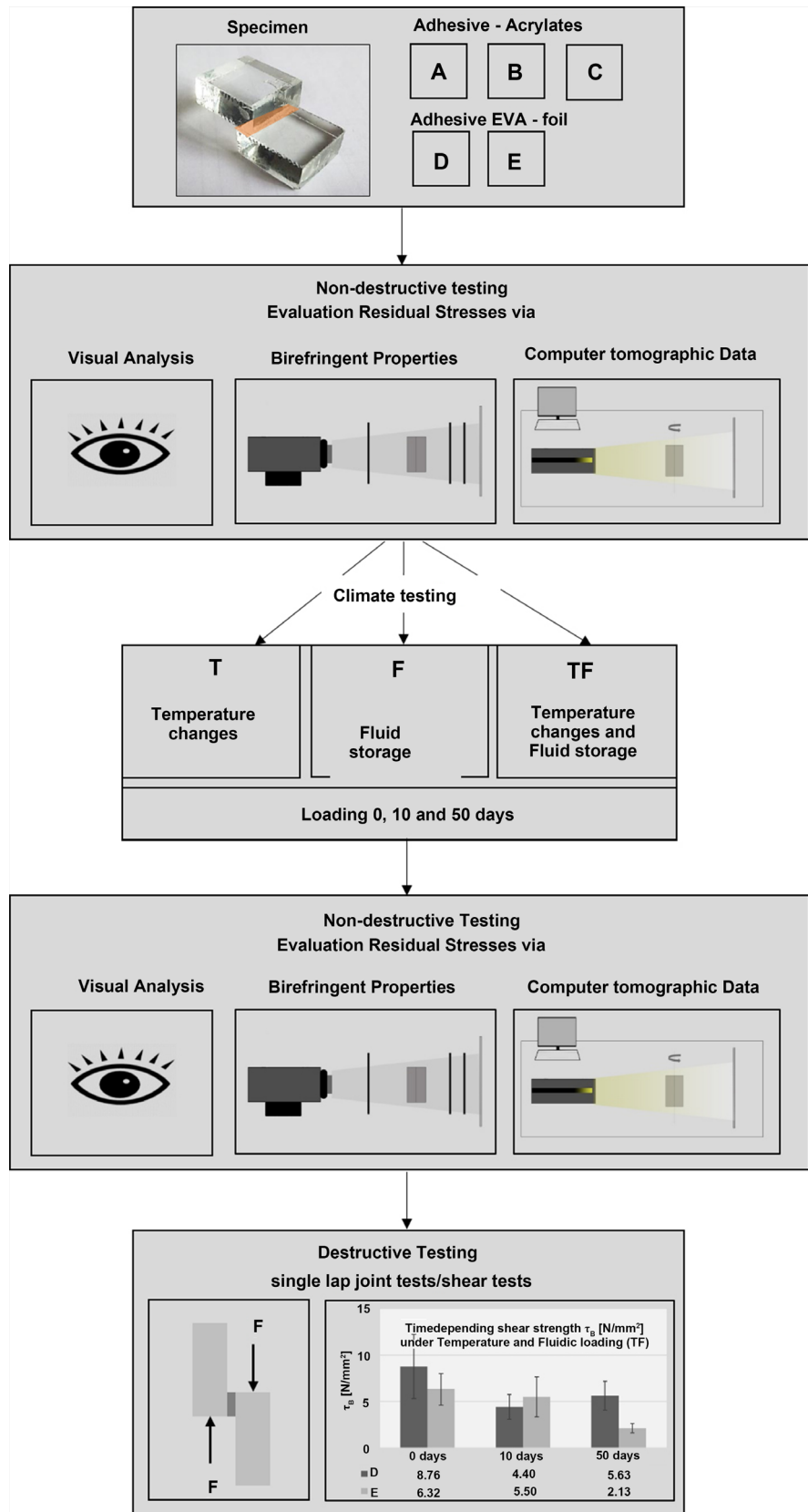
Figure 2. Experimental approach for the evaluation of long-term behavior of bonded glass panes.
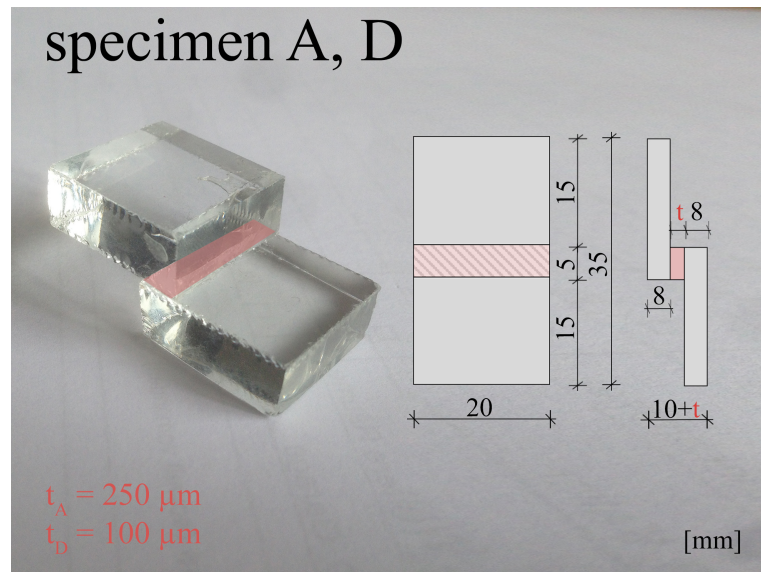
Figure 3. Test specimen for series A and D.

ambient temperatures. Since all materials/components are in direct contact with the fluid (glycol mixture), this is an additional influence to be considered. For this reason, three different climate settings are defined:

- alternating thermal stress (T)
- fluidic storage (F)
- alternating thermal stress in combination with fluidic storage (TF)

The temperature regime for the thermal loading is chosen according to DIN EN 1942 [16] and ETAG 002 [19]. The temperature ranges between −20°C and +80°C in a time span of 21 h. During one cycle the temperature idles at −20°C, +40°C and +80°C. The circulating fluid (glycol mixture) in the capillary glasses is used as a storage medium for the specimen. Each specimen of tests with fluidic influence (F) and combined loading (TF) is stored separately. Depending on the test series, the destructive and non-destructive tests are performed after 10 or 50 days of loading. Computed tomographic analyses are conducted on samples loaded for 10 days. In addition, some lap joint tests are performed on specimen without any influence of artificial aging as reference.

Plastic materials are often used for bonding purposes. In this case, the aging process is not only influencing the bonding material itself but also the interface to the bonded components. From the practical and structural engineering point of view, plastic materials are often analyzed by destructive lap joint tests to obtain the structural behavior and corresponding stress-strain relationships, respectively. Analyzing the nature of fractures (brittle, ductile) as well as the interface layers after tests can provide valuable information on aging mechanisms and their influence on bonds. Applying non-destructive analyzing methods, the authors want to evolve und facilitate deeper comprehension of aging processes in artificial aging simulations. The visual analyses and the evaluation of birefringent properties representing optical retardations according to **Figure 2** are

conducted for all specimens. In addition, one specimen of each series is examined by computed tomography.

4. Evaluation Methods

For the non-destructive testing, three different methods are applied. At first, a visual analysis is executed being the simplest practical approach to assess the quality of the connection and especially the optical requirements according to Table 1. Afterwards, birefringent properties of the specimens are analyzed, representing a commonly used method for analyzing glass residual stresses after forming processes (bottles, pre-stress glass structures, etc.). The last step is the evaluation of computed tomographic data, which is the most financial- and time-consuming method. It promises additional information, since transparent mediums have not often been analyzed yet.

4.1. Visual Analysis

The condition of adhesive bonds is described and evaluated by photographs. Amongst others, the following phenomena and damage patterns, respectively, can be detected:

- detachment of the adhesive from the components (delamination)
- bubbles
- discoloration
- cloudiness
- geometry anomalies of the layering

The cloudiness of an adhesive after artificial aging does not necessarily indicate a critical loss of strength, however, the material does not meet the optical demands defined in Table 1. The specimens are evaluated in the overlapping zone as depicted in Figures 4(a)-(c) show the analyses of specimen A112 (acrylate) before and after artificial aging (TF). Before loading, the visual examination does not reveal any disturbance in the overlapping area (Figure 4(a)), while after 10 days of fluidic storage and alternating temperature loading, a slight cloudiness is detected appearing as grey dotted pattern (marked area in Figure 4(c)).

The photographs of specimen D97 (EVA) before and after artificial aging are shown in Figure 4(d) and Figure 4(e). In compliance to the acrylate, no conspicuity is detected previous to the aging process (Figure 4(d)). And even after 10 days of artificial aging (TF) no changes or damages are visibly recognizable (Figure 4(e)).

4.2. Birefringent Properties

In the case of unloaded optically isotropic materials (such as glass and transparent polymer materials), the refractive indices are constant in all directions. However, when stresses are induced by external loading or due to manufacturing constraints (e.g. residual or internal stresses due to shrinking effects), particle spacing changes at molecular level leading to dissimilar propagation
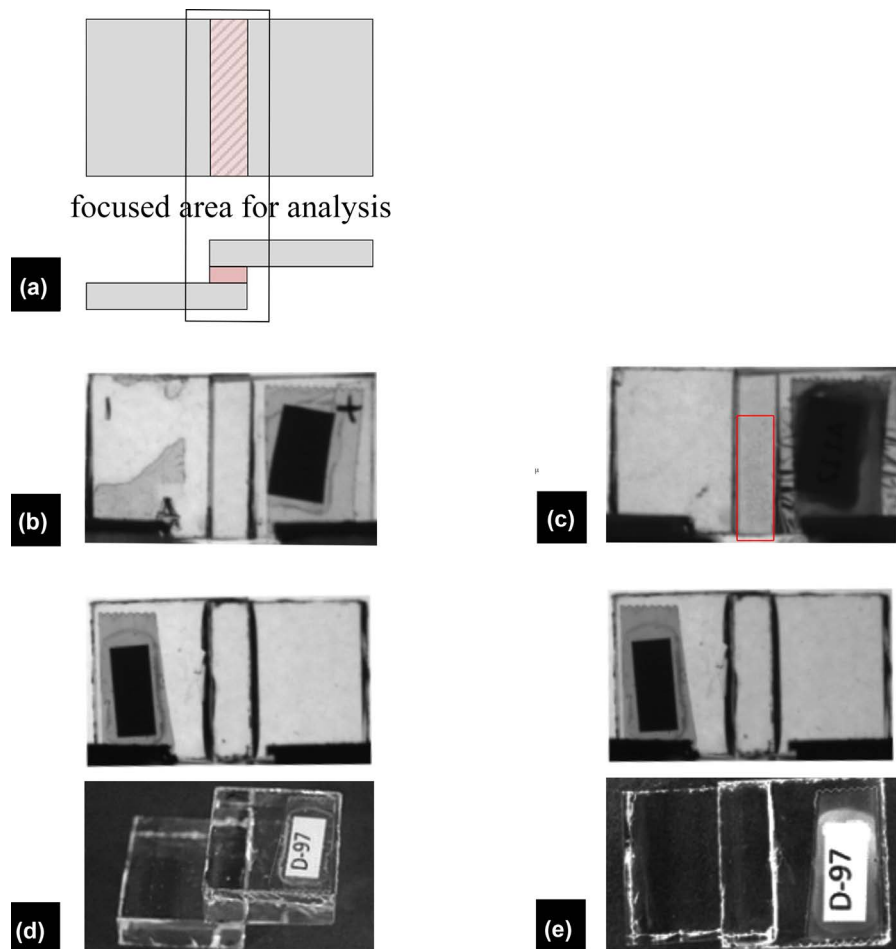
Figure 4. Visual analysis, (a) description of analyzed zone, (b) specimen A112—before climatic loading, (c) specimen A112—after climatic loading (10 days, TF), (d) specimen D97 before climatic loading, (e) specimen D97 after climatic loading (10 days, TF).

velocities of light for different spatial directions. When irradiated by polarized light, for example within a polarimeter, the light wave is split into two components running through the body at different speeds and therefore going along with a phase shift when exiting the specimen. This shift is referred to as optical retardation R [nm] and it gives a qualitative measure of the intrinsic stresses in the material (at constant sample thickness excluding birefringence). If R = 0, the system is at an optically isotropic state. The greater the optical path difference gets, the bigger the differences in the deflected light wavelengths and thus the stresses in the system are. However, only in exceptional cases, the size can be derived directly [20]. The method is therefore able to detect the qualitative distribution of the internal stresses.

Here, the birefringent properties of the lap joints are evaluated using a "StrainMatic M4/120" polarimeter from illis GmbH reflecting plane stress states. The lap joints are examined before and after artificial aging. Investigations of pure glass elements (non-overlapping area of lap joints) reveal no or a very low stress level (only at edges due to processing/cutting of glass components). In

Figure 5, the results of specimens A112 (acrylate) and D97 (EVA) are shown. The dark red and black areas are caused by the labelling of the specimens (for reasons of identification). They are not considered in the evaluation, only the overlapping zone is of importance (Figure 5(a)). Before artificial aging, specimen A112 shows certain stress differences in the lower bonding area (R ≈ 9.0 nm, Figure 5(b)). After aging of 10 days (TF), these differences disappear. The area of relaxation corresponds to the detected visual changes in Figure 4(c) (gray dotted area). An increase of stress differences is visible in the upper half of the bonding area.

For specimen D97, distinct stress differences (R ≈ 12.0 nm, Figure 5(d)) are visible in the total bonding area after the manufacturing process. After artificial aging of 10 days (TF), a slight decrease is noticeable (Figure 5(e)). This relaxation is not detectable in the visual analysis (Figure 4(e)).

4.3. Computed Tomographic Analysis

Computed tomography is a non-destructive imaging method to acquire 3-dimensional data from different specimens based on 2D-X-ray photographs. For this purpose, the object is irradiated from several directions starting at 0 and rotating to 360 degrees. In-between rotation stops, an X-ray picture is taken. Afterwards, all X-ray measurements are computed to a single volume data set. The number of pictures influences the quality of this set [21]. It contains voxel of different gray level, which mainly represent the attenuation of the X-ray beam at different positions. The attenuation depends on the material, the density, the thickness of material and the X-ray energy. The higher it is at a voxel position, the higher its gray level gets. Besides this favorable effect, undesirable effects called artefacts occur as well. Different artefacts have different causes, such as physical effects during the scan or the applied algorithms for reconstructing the data. To provide valid data from computed tomography it is important to reduce artefacts as good as possible and to identify remaining ones.

For the described experiments a *nanotom m* from *GE* is used. It runs with a 14-bit *GE DXR* detector with 3.072 × 2.400 pixel. To acquire and reconstruct the data, *phoenix datos|x* is applied and for the analysis and visualization of the data set, the software *VG Studio MAX* (*Volume Graphics*). For the scan the parameters listed in Table 4 are used.

These parameters applied to the described specimens lead to a resolution of 0.020888 mm in each direction, going along with corresponding minimum detectable details in this size. The resolution of the data set mainly depends on the size of the specimen and the used power. The higher the resolution, the better the detectability of small details.

Figure 6(a) shows a full 3D computed tomographic volume data set of a lap joint specimen. The round plate at the bottom is part of the specimen holding system in the CT and not relevant for the evaluation. Figure 6(b) and Figure 6(c) show the relevant cutting planes within the sample. With the help of the

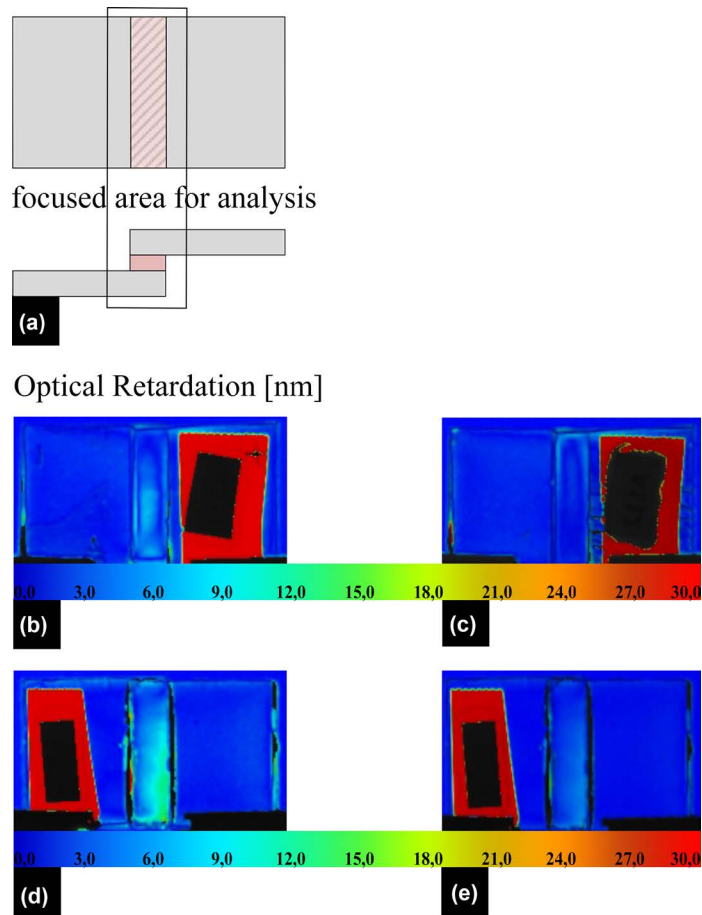(a)

Optical Retardation [nm]

(b) (c)

(d) (e)

Figure 5. Optical retardation, (a) description of analyzed area, (b) specimen A112—before climatic loading, (c) specimen A112—after climatic loading (10 days, TF), (d) specimen D97 before climatic loading, (e) specimen D97 after climatic loading (10 days, TF).
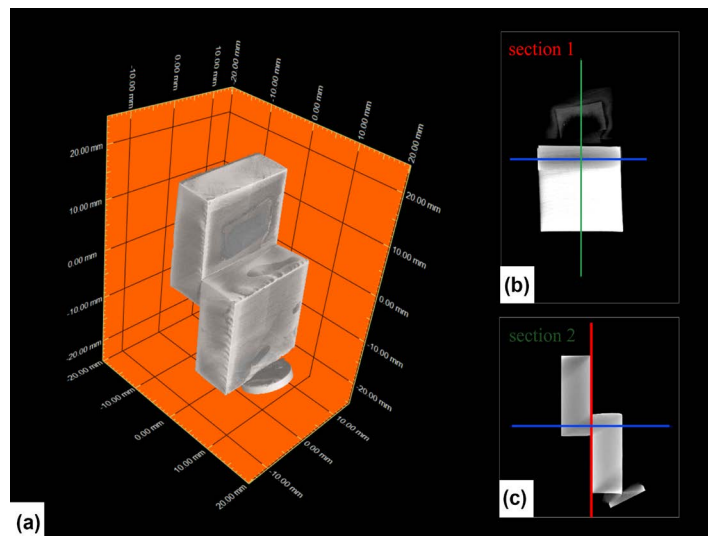

Figure 6. Computed tomographic data set, (a) full 3D CT scan of lap joint specimen, (b) analyzing section for evaluation of bonding layer (Section 1), (c) relevant section layer in middle of bonding layer.

Table 4. Parameters used in the CT scanning process.

Parameter	Value
Voltage	120 kV
Current	80 μA
Modus	1
Scan duration	1 hour
Target	Diamant
Number of pictures	1200

Section 1, the bonding is examined in the middle of the layer. As further representation, an integrated layer image with a thickness of 1 mm is produced: the gray values of all layer images (0.5 mm to the right and left of the cutting plane and in the middle of the adhesive layer) are summarized, averaged and represented as one image. With the help of this method, certain effects are to be clarified and compared with the representations of the visual analysis and representation of the optical retardation. In the reconstructed images, stripes are sometimes visible (see, for example, Figure 7(a)). These do not characterize different X-ray densities in the material but represent an artifact which frequently occurs in computed tomographic analyzes of vitreous bodies.

Specimen A112 does not show irregularities in the individual layer images within the bonding before loading (Figure 7(a) and Figure 7(b)). After an artificial aging process of 10 days (TF), small cracks are visible in the acrylate (Figure 7(c) and (Figure 7(d))) with length of 0.10 mm to 0.26 mm. In an enlargement, these cracks can be detected over the entire adhesive layer thickness (highlighted blue by threshold methods). In the integrated layer image these irregularities are also clearly visible (Figure 7(d)). The cracks revealed by the computed tomographic images are not recognizable in the visual analysis. They are an indication of the stress reduction, which is clearly detectable by the decrease of optical retardation (Figure 5(c)).

The computed tomographic image in the middle of the bonding layer of specimen D97 (Figure 8(a)) shows a certain lined structure (highlighted in dark blue). However, this phenomenon is not related to the material but based on artefacts. After the aging process of 10 days TF, it is not visible anymore. In comparison to specimen A112 (Figure 7(d)), the blue coloring in Figure 8(b) does not reveal any specific changes due to the climatic loading.

4.4. Destructive Testing

For reasons of validation regarding non-destructive test results, destructive lap joint tests on the specimens without and with aging effects are performed and presented in Figure 9 and Figure 10. The stress-strain-relations without aging effects are average curves determined from several tests of each series. However, the behavior with aging effects is the individual curve of the corresponding specimen (A112, D97).
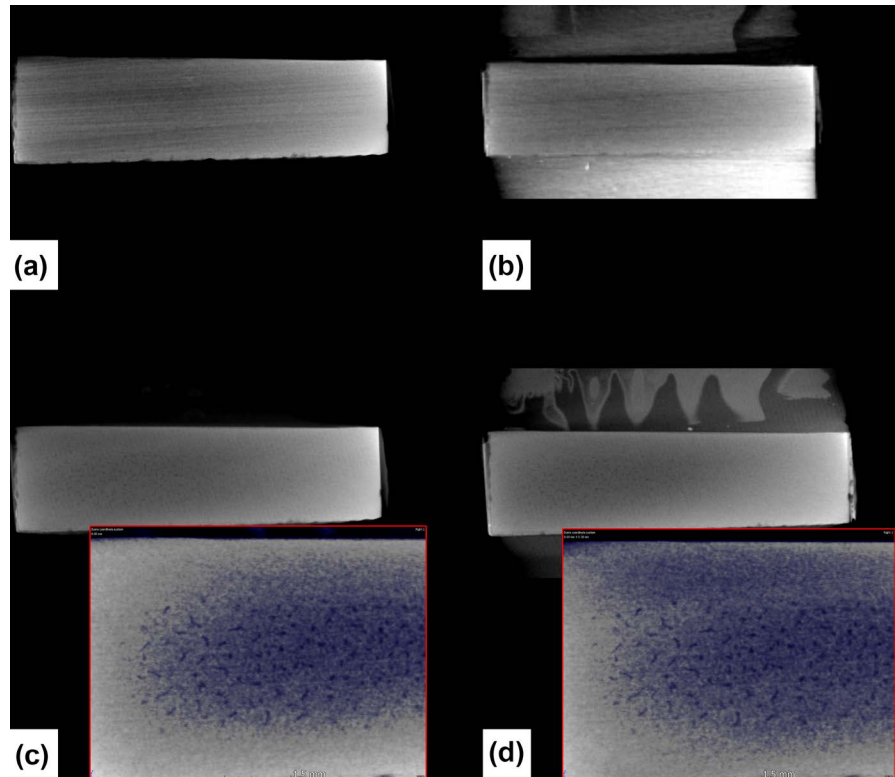
Figure 7. Computed tomographic images of specimen A112—computed tomographic data before (a) image in the middle of bonding layer, (b) average result over bonding layer) and after climate loading (TF) of 10 days, (c) middle of bonding layer, (d) average result over bonding layer with blue highlighting of density differences).
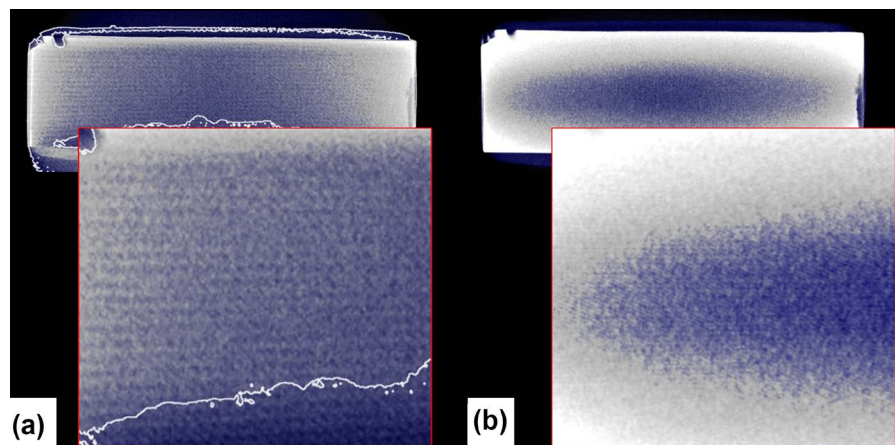

Figure 8. Computed tomographic images of specimen D97—computed tomographic data before (a) image in the middle of bonding layer) and after climate loading (TF) of 10 days (b) image in the middle of bonding layer with blue highlighting of density differences).

The connections bonded by acrylate A show a nonlinear material behavior without considering aging effects (**Figure 9**, without aging effects, average of specimen A). In comparison, specimen A112 behaves quite different after 10 days of artificial aging (TF). The material seems to show a certain embrittlement
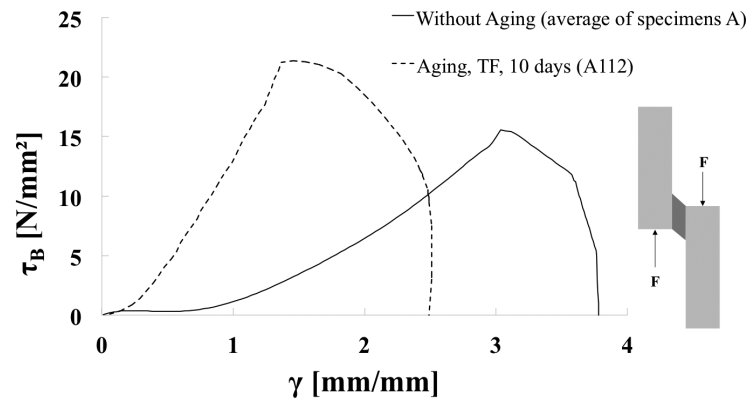
Figure 9. Lap join test—τ_B-γ diagram, bonding material A—without aging effects (average of series A) and with aging effect TF, 10 days (specimen A112).
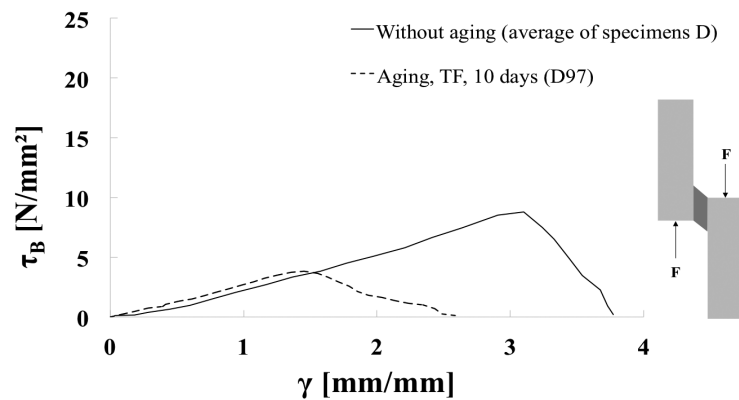

Figure 10. Lap join test—τ_B-γ diagram, bonding material D—without aging effects (average of series D) and with aging effect TF, 10 days (specimen D97).

over time—indicated by the decreased strain ability with a simultaneous increase of shear strength (**Figure 9**, Aging, TF, 10 days, specimen A112). This is also indicated by the results of the computed tomographic data (**Figure 7**): the small cracks point to this conclusion as well. The material behavior of different specimens in this series shows a wide variety regarding stiffness as well as shear strength under aging effects. Furthermore, the failure mode is not consistent—both, cohesion and adhesion failures are observed. The aging under temperature changes and fluidic storage seems to have diverse influences on the material. However, a cause investigation of the phenomenological effects is not accomplishable using the described methods and not subject of this research.

Figure 10 shows the results of specimens with bonding material D. Without the influence of artificial aging, the stiffness behavior of the joint before failure can be described as quasi linear (**Figure 10**, without aging effect, average of specimen D). After artificial aging TF of 10 days, specimen D97 shows a distinct decrease of shear strength (**Figure 10**, Aging, TF, 10 days, D97) at a similar stiffness level. Different specimens under aging influences in this series show a

wide variety of shear strength, however, stiffness levels are always quite equal. As failure modus, an adhesion failure is observed for all specimens in this series. It seems that the artificial aging has negative influence on the bonding (adhesion forces) in the interface layer. Specific influences leading to this failure cannot be detected in the computed tomographic data (Figure 8). However, with the analysis of birefringent properties a decrease of optical retardation (Figure 6) is visible.

5. Results

Based on the analyzed samples of all testing series, Table 5 assesses the detection quality of various damage phenomena. Computed tomographic images provide more detailed information of phenomena already detectable with the visual analysis. The evaluation of the optical retardation gives very general information on current states of bonding layers. With the 2D picture a specification where stress changes over the thickness of the specimen occur is not possible. With a full 3D CT scan, this lack of information can be closed. Moreover, destructive testing is very important to evaluate the detected phenomena. Important information can be derived from testing to connect material phenomena to mechanical behavior.

Regarding the polymers tested, damage is already evident after 10 days under combined loading of fluidic storage and temperature gradients. For acrylate A as bonding layer, the damage is clearly visible using CT images and it is verified in the destructive testing as well. For bonding material D, less aging influences are visible in the presented non-destructive testing methods. However, the influence on the mechanical behavior (especially the strength) is obvious.

Based on the assigned task, choosing suitable materials for bonding glass devices (Figure 1), material D is chosen. Albeit mechanical changes due to the aging process can be detected, the specimen shows very high optical stability over the testing time.

6. Conclusions

In this contribution, acrylate and EVA materials for bonding glass panes are examined under the aspects of optical and mechanical requirements (Table 1). Bonded and artificially aged specimens are analyzed with three different non-destructive testing methods (visual, birefringent properties, computed tomography) to evaluate influences of aging processes on the connection. In addition, destructive tests are performed.

Computed tomographic analyses can be used to detect specific effects at an early stage. For the acrylate test specimen A112 small cracks in the bonding layer become visible with the help of the CT images already after 10 days of artificial aging influencing stiffness and resistance. Measurements with the polarimeter show significant reductions in the optical retardation in bonding layer; however, only with the CT information it is possible to draw conclusions to the cause (cracks). The computed tomographic images of the EVA specimen D97 do not

Table 5. Evaluation of non-destructive testing methods on transparent connections under climatic loading.

	Visual Analysis	Analysis of birefringent properties	Computed tomographic data
Delamination	++	−	+
Clouding	++	−	+
cracks (Adhesive A)	−	−	++
Anomalies in geometry	++	+	++
Residual stresses	o	++	o

detection of damage mechanism with non-destructive testing methods after artificial aging (10 days TF) (++ very good, + good, o not possible, − bad).

exemplify changes in the bonding layer. Here, the decrease in shear strength is effected by the interface layer between glass and EVA film. These results are confirmed by destructive tests.

All methods presented are somehow useful for the phenomenological detection of aging effects on transparent bonds. However, the detectable phenomena differ and depending on the method, the density of information is quite different. Computed tomographic images can provide detailed information on aging phenomena. However, CT analyses are time-consuming, costly, applicable only to limited sizes of specimens and therefore not addressed in practical applications and investigations in general. By evaluating the destructive and non-destructive analyses, damage pattern of bonded connections can be identified and taken into account for improved material models of numerical simulations leading to optimized approximation of mechanical behavior.

Acknowledgements

References

[1] Comission, E. (2016) Buildings.
https://ec.europa.eu/energy/en/topics/energy-efficiency/buildings

[2] Heiz, B.P.V., Pan, Z., Lautenschläger, G., Sirtl, C., Kraus, M. and Wondraczek, L. (2017) Smart Windows: Ultrathin Fluidic Laminates for Large-Area Façade Integration and Smart Windows. *Advanced Science*, **4**.
http://onlinelibrary.wiley.com/doi/10.1002/advs.201600362/full

[3] Heiz, B.P.V., Pan, Z., Su, L., Le, S.T. and Wondraczek, L. (2018) A Large-Area Smart Window with Tunable Shading and Solar-Thermal Harvesting Ability Based on Remote Switching of a Magneto-Active Liquid. *Advanced Sustainable Systems*, **2**. http://onlinelibrary.wiley.com/doi/10.1002/adsu.201700140/full

[4] Folienwerk Wolfen GmbH (2016) Allgemeine bauaufsichtliche Zulassung Z-70.3-238.
http://www.folienwerk-wolfen.de/fileadmin/upload/downloads/Glass-lamination_fi

lms/20161014_ABZ_evguard_Seite1.pdf

[5] Siebert, G. and Maniatis, I., Eds. (2012) Tragende Bauteile aus Glas—Grundlagen, Konstruktion, Bemessung, Beispiele. [Load-Bearing Glass Components—Basics, Design Dimensioning, Examples.] Ernst&Sohn, Berlin.

[6] Schott Technical Glass Solutions GmbH (2015) Schott Xensation Cover. http://www.schott.com/d/xensation/a3f53d0a-586e-41b6-830c-48329da352c7/1.0/schott_xensation_cover_db_row.pdf

[7] Sirtl, C., Kraus, M., Hadlich, C., Osburg, A. and Wondraczek, L. (2017) Zur Bewertung klimatisch beanspruchter geklebter Glasverbindungen. [For the Evaluation of Climatically Stressed Bonded Glass/Glass Connections.] *ce/papers*, **1**, 254-275. http://onlinelibrary.wiley.com/doi/10.1002/cepa.26/full

[8] Folienwerk Wolfen GmbH (2018) The Clever Laminating Film. http://www.evguard.net/de/

[9] DELO Industrie Klebstoffe (2014) Delo Photobond GB 310. https://www.delo-adhesives.com/fileadmin/datasheet/DELO%20PHOTOBOND_GB310_%28TIDB-GB%29.pdf

[10] Folienwerk Wolfen GmbH (2017) Technical Data Sheet. http://www.folienwerk-wolfen.de/fileadmin/upload/downloads/Glass-lamination_films/2017-08_Technical-Data_evguard_EN.pdf

[11] DIN Deutsches Institut für Normung e.V. (2009) Klebstoffe—Bestimmung der Zugscherfestigkeit von Überlappungsklebungen (DIN EN 1465:2009-07) [Adhesives—Determination of Tensile Lap-Shear Strength on Bonded Assemblies]. Beuth Verlag GmbH, Berlin.

[12] DIN Deutsches Institut für Normung e.V. (2011) Strukturklebstoffe—Bestimmung des Scherverhaltens struktureller Klebungen (DIN EN 14869:2011-07) [Structural Adhesives—Determination of Shear Behavior of Structural Bonds]. Beuth Verlag GmbH, Berlin.

[13] DELO Industrie Klebstoffe (2014) DELO Norm 5—Bestimmung von Druckscherfestigkeiten [DELO Guideline 5—Determination of Compressive Shear Strength]. DELO Industrie Klebstoffe, Windach.

[14] DIN Deutsches Institut für Normung e.V. (2012) Begriffe auf dem Gebiet der Alterung von Materialien—Polymere Werkstoffe (DIN 50035:2012-09) [Terms and Definitions Used on Ageing of Materials—Polymeric Materials]. Beuth Verlag GmbH, Berlin.

[15] Ehrenstein, G.W. and Pongratz, S. (2007) Beständigkeit von Kunststoffen [Resistance of Plastics]. Carl Hanser Fachverlag, München. https://doi.org/10.3139/9783446411494

[16] DIN Deutsches Institut für Normung e.V. (2004) Klebstoffe—Auswahlrichtlinien für Labor-und Alterungsbedingungen zur Prüfung von Klebverbindungen (DIN EN ISO 9142:2003) [Adhesives—Guide to the Selection of Standard Laboratory Ageing Conditions for Testing Bonded Joints]. Beuth Verlag GmbH, Berlin.

[17] DIN Deutsches Institut für Normung e.V. (2013) Kunststoffe—Künstliches Bestrahlen oder Gewittern in Geräte—Teil 2: Xenonbogenlampen (DIN EN ISO 4892-2:2013-06) [Plastics—Methods of Exposure to Laboratory Light Sources—Part 2: Xenon-arc lamps]. Beuth Verlag GmbH, Berlin.

[18] DIN Deutsches Institut für Normung e.V. (1992) Alterung von Kfz-Bauteilen in Sonnensimulationsanlagen (DIN 75220:1992-11) [Ageing of Automotive Components in Solar Simulation Units]. Beuth Verlag GmbH, Berlin.

[19] Bundesministerium für Verkehr, Bau und Stadtentwicklung (1998) Bekanntma-chung der Leitlinie für die Europäische Technische Zulassung für geklebte Glaskonstruktionen—Teil 1: Gestützte und ungestützte Systeme (ETAG 002) [Structural Sealant Glazing Systems—Part 1: Supported and Unsupported Systems]. Beuth Verlag GmbH, Berlin.

[20] Katte, H. (2008) Bildgebende Messung der Spannungsdoppelbrechung in optischen Materialien und Komponenten [Imaging Measurement of Stress Birefringence in Optical Materials and Components]. Photonik, 05/2008, 60-63.
http://www.ilis.de/de/pdf/photonik_2008_05_60.pdf

[21] Biermann, H. and Krüger, L. (2015) Moderne Methoden der Werkstoffprüfung [Modern Methods for Material Testing]. Wiley-VCH, Weinheim.